Finite two-dimensional oscillator: II. The radial model

2001 J. Phys. A: Math. Gen. 34 9399

(http://iopscience.iop.org/0305-4470/34/44/305)

INSTITUTE OF PHYSICS PUBLISHING JOURNAL OF PHYSICS A: MATHEMATICAL AND GENERAL

J. Phys. A: Math. Gen. **34** (2001) 9399–9415 PII: S0305-4470(01)26598-6

Finite two-dimensional oscillator: II. The radial model

Natig M Atakishiyev[1], George S Pogosyan[2,3], Luis Edgar Vicent[1,2] and Kurt Bernardo Wolf[2]

[1] Instituto de Matemáticas, UNAM, Apartado Postal 273-3, 62210 Cuernavaca, Morelos, México
[2] Centro de Ciencias Físicas, Universidad Nacional Autónoma de México, Apartado Postal 48-3, 62251 Cuernavaca, Morelos, México

Received 6 July 2001
Published 26 October 2001
Online at stacks.iop.org/JPhysA/34/9399

Abstract

A finite two-dimensional radial oscillator of $(N+1)^2$ points is proposed, with the dynamical Lie algebra $so(4) = su(2)_x \oplus su(2)_y$ examined in part I of this work, but reduced by a subalgebra chain $so(4) \supset so(3) \supset so(2)$. As before, there are a finite number of energies and angular momenta; the Casimir spectrum of the new chain provides the integer radii $0 \leqslant \rho \leqslant N$, and the $2\rho+1$ discrete angles on each circle ρ are obtained from the finite Fourier transform of angular momenta. The wavefunctions of the finite radial oscillator are $so(3)$ Clebsch–Gordan coefficients. We define here the Hankel–Hahn transforms (with dual Hahn polynomials) as finite-N unitary approximations to Hankel integral transforms (with Bessel functions), obtained in the contraction limit $N \to \infty$.

PACS numbers: 02.20.Qs, 02.30.Gp, 42.30.Kq, 42.30.Va

1. Introduction

In part I of this work [1], the finite two-dimensional Cartesian oscillator was characterized as the direct product of two finite one-dimensional oscillators. In this second part, we abstract the postulates we proposed and the results we obtained, into a Lie-algebraic structure, which includes mode number and angular momentum, as well as radial position and angle among the observables. The range of values of these observables will be given by the spectra of certain operators that provide the irreducible representation (irrep) labels of subalgebras along two reduction chains. The range of the observables is a finite number of equidistant points when the algebra is compact.

As we saw in part I, the finite one-dimensional oscillator has a dynamical algebra $u(2) = u(1) \oplus su(2)$ [2,3], familiar from angular momentum theory. The positions and mode numbers are the eigenvalues of two of the generators, $Q = J_1$ and $H = J_3 + E_J + \frac{1}{2}\hat{1}$, where

[3] Permanent address: Laboratory of Theoretical Physics, Joint Institute for Nuclear Research, Dubna, Russia.

0305-4470/01/449399+17$30.00

$E_J = j\hat{1}$ is the $u(1)$ central algebra which gives the $su(2)$ irrep label j for a finite oscillator of $2j+1$ points. Two such independent oscillators (on orthogonal directions labelled x and y with the same number of points) provided a Cartesian direct-sum system characterized by the algebra $u(1) \oplus su(2)_x \oplus su(2)_y$. But in two dimensions the accident occurs that $su(2) \oplus su(2) = so(4)$. We propose here to reformulate the second postulate of D-dimensional (finite or standard quantum) harmonic oscillators in the following, more general terms:

(1) There exists a *position* subalgebra, with an (algebraic) basis of generators $\vec{Q} \stackrel{\text{def}}{=} (Q_x, Q_y, \ldots, Q_D)$. The Casimir operator of this subalgebra provides the irrep labels, whose values are the radii in the system.

(2) There exists one (self-adjoint and compact) *Hamiltonian* operator H, which is the generator of time evolution; it satisfies the vector Newton–Lie or Hamilton–Lie equations (*verbatim* from part I):

$$[H, [H, \vec{Q}]] = \vec{Q} \quad \Longleftrightarrow \quad \begin{cases} [H, \vec{Q}] \stackrel{\text{def}}{=} -\mathrm{i}\vec{P} \\ [H, \vec{P}] = \mathrm{i}\vec{Q}. \end{cases} \tag{1}$$

The first Hamilton equation is purely geometrical: it only defines the *momentum* subalgebra, containing $\vec{P} \stackrel{\text{def}}{=} (P_x, P_y, \ldots, P_D)$. The second Hamilton equation contains the dynamics of the oscillator.

Here we add a statement for orbital angular momentum:

(2 bis) In D dimensions, there exists an *angular momentum* subalgebra $so(D)$ of generators $\mathrm{span}\{M_{\alpha,\beta}\}$ $(1 \leqslant \alpha < \beta \leqslant D)$ that commute with H, and under which $\vec{Q}$, and hence $\vec{P}$, transform as D-vectors:

$$\begin{aligned} [M_{\alpha,\beta}, Q_\gamma] &= -\mathrm{i}(\delta_{\beta,\gamma} Q_\alpha - \delta_{\alpha,\gamma} Q_\beta) \\ [M_{\alpha,\beta}, P_\gamma] &= -\mathrm{i}(\delta_{\beta,\gamma} P_\alpha - \delta_{\alpha,\gamma} P_\beta) \end{aligned} \qquad [M_{\alpha,\beta}, H] = 0. \tag{2}$$

(3) Under Lie brackets, all operators ($\vec{Q}$, $\vec{P}$, H, $\hat{1}$ and $M_{\alpha,\beta}$) close into a Lie algebra.

In [4] we saw that a number of Lie algebras (and q-algebras) can satisfy postulate (3). In searching for a compact algebra that solves the $D = 2$ case of our immediate concern, we emphasize that the Lie brackets between the components of the position and momentum operators need not be the familiar Heisenberg–Weyl ones ($[Q_\alpha, P_\beta] = \mathrm{i}\delta_{\alpha,\beta}\hat{1}$), nor even that the components of position and momentum commute amongst themselves ($[Q_\alpha, Q_\beta] = 0 = [P_\alpha, P_\beta]$), as they do in the Cartesian model of the finite oscillator of part I. In this paper we propose the Lie algebra $so(4)$ to model the finite two-dimensional oscillator with discrete radial and angular coodinates. The choice is natural because it is the same algebra (and representation) used in part I for the same system; moreover, it indicates that in dimension D the algebra will be $so(D+2)$.

In section 2 we organize the satisfaction of the three (+ bis) finite oscillator postulates (1) and (2) for the one- and two-dimensional cases. With the aid of *ad hoc* patterns, the generators of the orthogonal groups can be handled easily. In section 3 we identify the subalgebra chains that define eigenbases of mode and angular momentum (n, m), and of radius and angular momentum (ρ, m). The overlaps yield the wavefunctions, which turn out to be the $so(3)$ Clebsch–Gordan coefficients, as shown in section 4. In section 5 we use the ordinary discrete Fourier transform to pass between multiplets of angular momentum states to a Kronecker basis of points on a circle. The finite oscillator position space will thus have discrete radii $\rho \in \{0, 1, \ldots, N\}$ and angles θ_k, $k \in \{-\rho, -\rho+1, \ldots, \rho\}$—a total of $(N+1)^2$ points.

In the same way that the isotropic Fourier transform decomposes into a direct sum of Hankel (or Fourier–Bessel) transforms for angular momenta $m \in \{0, \pm 1, \pm 2, \ldots\}$, in

section 6 we decompose the finite oscillator evolution into Hankel–*Hahn* transforms with $m \in \{0, \pm 1, \ldots, \pm N\}$. We call them so because their kernel contains the finite dual Hahn orthogonal polynomials. The Hankel–Hahn transform of a mode-n state multiplies it by $(-\mathrm{i})^n$, as it should. As we show in section 7, the $N \to \infty$ limit matches the results of the usual two-dimensional quantum oscillator. Some conclusions are offered in section 8.

2. The $so(4)$ algebra of the finite oscillator

The dynamical Lie algebras of the one- and two-dimensional finite oscillators are $su(2) = so(3)$ and $su(2) \oplus su(2) = so(4)$ respectively, plus a one-dimensional centre $u(1)$. Finite oscillators of higher dimension are posited to stem from $so(D)$, so it will be convenient to use a uniform notation for the orthogonal algebras. As a simple guide, recall the standard realization of the generators of rotations in a space $\vec{z} \in \mathrm{Re}^D$, $\partial_\alpha \stackrel{\text{def}}{=} \partial/\partial z_\alpha$; it is $\Lambda_{\alpha,\beta} = -\mathrm{i}(z_\alpha \partial_\beta - z_\beta \partial_\alpha) = -\Lambda_{\beta,\alpha}$, $1 \leqslant \alpha < \beta \leqslant D$. The commutation relations that characterize the Lie algebra $so(D)$ are then

$$[\Lambda_{\alpha,\beta}, \Lambda_{\gamma,\epsilon}] = \mathrm{i}(\delta_{\alpha,\gamma}\Lambda_{\beta,\epsilon} + \delta_{\beta,\epsilon}\Lambda_{\alpha,\gamma} + \delta_{\epsilon,\alpha}\Lambda_{\gamma,\beta} + \delta_{\gamma,\beta}\Lambda_{\epsilon,\alpha}) \tag{3}$$

independently of the realization of its generators.

2.1. One-dimensional case

The one-dimensional finite oscillator (see [1, 3, 5]) has no angular momentum. The model has $u(2) = u(1) \oplus su(2) = so(2) \oplus so(3)$ for its dynamical Lie algebra instead. The central subalgebra $u(1) = so(2)$ has a single generator E_J, which is $j\hat{1}$ in the irrep j of $so(3)$, for a finite oscillator of $2j + 1$ points; since this number is fixed, it is often convenient to work simply with $so(3)$. Thus, position Q, momentum P and Hamiltonian H are identified through the pattern we introduced in [6], which arranges the $so(3)$ (and generally $so(D)$) generators:

$$\begin{array}{|c|c|} \hline \Lambda_{1,2} & \Lambda_{1,3} \\ \hline & \Lambda_{2,3} \\ \hline \end{array} \quad = \quad \begin{array}{|c|c|} \hline J_3 & -J_2 \\ \hline & J_1 \\ \hline \end{array} \quad = \quad \begin{array}{|c|c|} \hline H - j - \frac{1}{2} & P \\ \hline & Q \\ \hline \end{array} \tag{4}$$

From (3) and (4), the commutation relations of the J_α's are the standard

$$[J_1, J_2] = \mathrm{i}J_3 \qquad [J_2, J_3] = \mathrm{i}J_1 \qquad [J_3, J_1] = \mathrm{i}J_2 \qquad [E_J, J_k] = 0. \tag{5}$$

The Casimir invariant is $J^2 = J_1^2 + J_2^2 + J_3^2$ and has the spectrum $j(j+1)$, $j \in \{0, \frac{1}{2}, 1, \frac{3}{2}, \ldots\}$. $\left(\text{If needed, one could write } E_J = -\frac{1}{2} + \sqrt{J^2 + \frac{1}{4}}.\right)$ The dynamical quantities of the finite model obey

$$[Q, P] = \mathrm{i}(H - j - \tfrac{1}{2}) \qquad [H, P] = \mathrm{i}Q \quad [H, Q] = -\mathrm{i}P. \tag{6}$$

As detailed in part I, two subalgebra chains $so(3) \supset so(2)$ are of interest: that of position, where $Q = J_1$ is diagonal, and that of mode number (or energy), where H and J_3 are diagonal. We use the label $N = 2j$ to describe finite oscillators of $N + 1$ points and modes, writing thus

$$\begin{array}{ll} E_J\,|N; q\rangle_1 = \frac{1}{2}N\,|N; q\rangle_1 & E_J\,|N; n\rangle_{\mathrm{H}} = \frac{1}{2}N\,|N; n\rangle_{\mathrm{H}} \\ Q\,|N; q\rangle_1 = q\,|N; q\rangle_1 & H\,|N; n\rangle_{\mathrm{H}} = (n + \frac{1}{2})\,|N; n\rangle_{\mathrm{H}} \\ \text{position: } q|_{-N/2}^{N/2} & \text{mode number: } n|_0^N. \end{array} \tag{7}$$

The two bases are related through a rotation by $\frac{1}{2}\pi$ around the 2-axis, $e^{-i\frac{1}{2}\pi J_2} J_3 e^{i\frac{1}{2}\pi J_2} = J_1$; it follows that the kets $j = \frac{1}{2}N$ transform as

$$e^{-i\frac{1}{2}\pi J_2} : |N; n\rangle_H = |N; n-j\rangle_1 = \sum_{n'=0}^{2j} |N; n'\rangle_H \, d^j_{n'-j;n-j}(\tfrac{1}{2}\pi) \tag{8}$$

with a Wigner little d function [1, 7–10]. The finite oscillator 'Kravchuk' wavefunctions on $N+1$ points are defined by [5]

$$\Phi^{(N)}_n(q) = {}_1\langle N; q|N; n\rangle_H = {}_H\langle N; q+j|e^{+i\frac{\pi}{2}J_2}|N; n\rangle_H \tag{9}$$

$$= d^j_{q,n-j}(-\tfrac{1}{2}\pi) = d^j_{n-j,q}(\tfrac{1}{2}\pi). \tag{10}$$

They are orthonormal and complete over positions $q \in \{-j, -j+1, \ldots, j\}$ and modes $n \in \{0, 1, \ldots, 2j\}$.

2.2. Radial two-dimensional case

We generalize the asignment pattern (4) between dynamical observables and generators of the $so(4)$ algebra to include the angular momentum generator M with the commutators specified in (2) by postulate (2 bis). We introduce $J \stackrel{\text{def}}{=} H - E_J - \hat{1}$ (to play the role of $J_3 = H - E_J - \frac{1}{2}\hat{1}$ in the one-dimensional case) and organize the six generators $\Lambda_{\alpha,\beta}$, $1 \leqslant \alpha < \beta \leqslant 4$, into the following pattern [6]:

$$\begin{array}{|c|c|c|} \hline \Lambda_{1,2} & \Lambda_{1,3} & \Lambda_{1,4} \\ \hline & \Lambda_{2,3} & \Lambda_{2,4} \\ \cline{2-3} & & \Lambda_{3,4} \\ \cline{3-3} \end{array} \quad = \quad \begin{array}{|c|c|c|} \hline J & P_x & P_y \\ \hline & Q_x & Q_y \\ \cline{2-3} & & M \\ \cline{3-3} \end{array} \tag{11}$$

This pattern shows at a glance the commutation relations (3): the commutator of two generators on the same row (resp. column) is in the intersection of their columns (resp. rows)—after one of them is reflected across the diagonal by $\Lambda_{\alpha,\beta} = -\Lambda_{\beta,\alpha}$. A generator $\Lambda_{\alpha,\beta}$ will commute with all other $\Lambda_{\gamma,\delta}$'s that are outside its row α and column β (and their reflections across the diagonal, as column α and row β).

In the pattern (11) we see the following desirable properties: angular momentum M and mode (shifted energy) J commute; position (Q_x, Q_y) and momentum (P_x, P_y) transform as 2-vectors under angular momentum M; and x phase space (Q_x, P_x) and y phase space (Q_y, P_y) rotate similarly under the Hamiltonian and J. (Note that we are *not* introducing any 'angle' operator; the discrete angular coordinate will appear in section 5 through the finite Fourier transform of the angular momentum states.) On the other hand, there are also new 'non-standard' commutators $[Q_x, Q_y]$ and $[P_x, P_y]$ that generalize (6) to two dimensions, but which will need some interpretation to show that they are natural to the radial model. More generally, they are

$$[Q^{(\phi)}, P^{(\phi)}] = i\,J \qquad Q^{(\phi)} \stackrel{\text{def}}{=} e^{-i\phi M} Q_x e^{+i\phi M} \qquad P^{(\phi)} \stackrel{\text{def}}{=} e^{-i\phi M} P_x e^{+i\phi M} \tag{12}$$

$$[R^{(\theta)}_x, R^{(\theta)}_y] = iM \qquad R^{(\theta)}_x \stackrel{\text{def}}{=} e^{-i\theta J} Q_x e^{+i\theta J} \qquad R^{(\theta)}_y \stackrel{\text{def}}{=} e^{-i\theta J} Q_y e^{+i\theta J}. \tag{13}$$

The equivalence set of commutators (12) indicates that, on any direction ϕ of space ($Q^{(\phi)} = Q_x \cos\phi + Q_y \sin\phi$ in two dimensions), the commutator of collinear position and momentum is J; this is the 'finite oscillator form' (6). The second non-standard commutator (13)

of the radial oscillator model, in particular $[Q_x, Q_y]$, was zero in the *Cartesian* oscillator model of part I; in the present radial model, the components of any vector in phase space ($R_\alpha^{(\theta)} = Q_\alpha \cos\theta + P_\alpha \sin\theta$, $\alpha = x, y$) close into an $so(3)$ Lie subalgebra with the angular momentum operator M. As can be seen in the pattern (11), only $[Q_x, P_y] = 0 = [Q_y, P_x]$ commute or, more generally, $[Q^{(\phi)}, P^{(\phi+\frac{1}{2}\pi)}] = 0 = [R_x^{(\theta)}, R_y^{(\theta+\frac{1}{2}\pi)}]$.

3. Subalgebra chains of mode and position

In this section we prepare some mathematical results from the theory of orthogonal groups for the finite radial oscillator model.

3.1. Symmetric representations of $so(4)$

To analyse the subalgebra chains and overlaps that we shall use below, it is useful to recall the direct sum of two $so(3)$ algebras, labelled a and b, into an $so(4)$ algebra [11]. Using the patterns (4) and (11), it is

$$\begin{array}{|c|c|}\hline J_3^{(a)} & -J_2^{(a)} \\ \hline J_1^{(a)} \\ \cline{1-1}\end{array} \oplus \begin{array}{|c|c|}\hline J_3^{(b)} & -J_2^{(b)} \\ \hline J_1^{(b)} \\ \cline{1-1}\end{array} = \begin{array}{|c|c|c|}\hline J_3^{(a)}+J_3^{(b)} & -J_2^{(a)}-J_2^{(b)} & J_1^{(a)}-J_1^{(b)} \\ \hline J_1^{(a)}+J_1^{(b)} & J_2^{(a)}-J_2^{(b)} \\ \cline{1-2} J_3^{(a)}-J_3^{(b)} \\ \cline{1-1}\end{array} \qquad (14)$$

We work here with the further restriction that the representation of $so(4)$ be of the *symmetric* (or *most degenerate*) kind, whose commuting $so(3)$ Casimir operators are bound by

$$(\vec{J}^{(a)})^2 = E_J(E_J + \hat{1}) = (\vec{J}^{(b)})^2. \qquad (15)$$

This is inspired by the finite two-dimensional Cartesian array of part I, which is a square of $(N+1) \times (N+1)$ points. If the array were not square, polar (radius and angle) coordinates could be a bad choice (and we would propose elliptic coordinates instead).

In the symmetric $so(4)$ representations, the two independent second-degree Casimir operators are restricted to

$$\begin{aligned} \mathcal{C} &= \sum_{j,k} \Lambda_{j,k}\,\Lambda_{j,k} = 2(\vec{J}^{(a)})^2 + 2(\vec{J}^{(b)})^2 \\ &= 4j(j+1) = N(N+2) \qquad \text{where} \quad N \stackrel{\text{def}}{=} 2j \qquad (16) \\ \mathcal{D} &= \textstyle\sum_{j,k,l} \Lambda_{j,k}\Lambda_{l,4} = 2(\vec{J}^{(a)})^2 - 2(\vec{J}^{(b)})^2 = 0. \qquad (17) \end{aligned}$$

Hence the value of $N = 2j \in \{0, 1, 2, \ldots\}$ is sufficient to characterize the symmetric $so(4)$ irreps, whose dimension is $(N+1)^2$.

3.2. States of mode and angular momentum

The eigenbasis of the two commuting $so(4)$ generators

$$J = \Lambda_{1,2} = J_3^{(a)} + J_3^{(b)} \qquad M = \Lambda_{3,4} = J_3^{(a)} - J_3^{(b)} \qquad (18)$$

is the set of finite radial oscillator states classified by mode (energy) and angular momentum (see the pattern (14) and equations (7)) by the subalgebra chains $so(4) \supset so(2)_{\mathrm{J}} \oplus so(2)_{\mathrm{M}} \simeq$

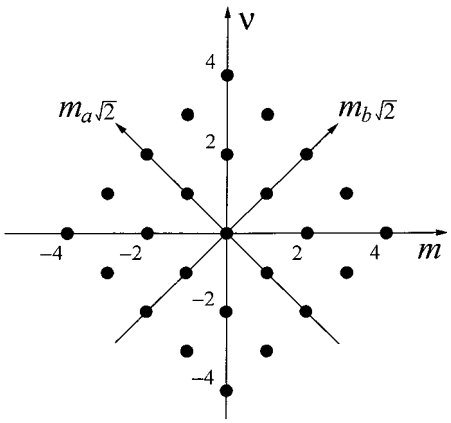

Figure 1. States $|N; \nu, m\rangle_{\rm JM}$ of the two-dimensional finite oscillator, classified by mode (∼energy) $\nu = m_a + m_b$ and angular momentum $m = m_a - m_b$, for $N = 4$ there are 25 states.

$u(1)_a \oplus u(1)_b$. When $J_3^{(a)}$ and $J_3^{(b)}$ have eigenvalues $m_a|_{-j}^{j}$ and $m_b|_{-j}^{j}$ respectively, the eigenstates will be denoted by

$$J|N; \nu, m\rangle_{\rm JM} = \nu|N; \nu, m\rangle_{\rm JM} \tag{19}$$

$$\nu = m_a + m_b \in \{-N, -N+1, \ldots, N\} \tag{20}$$

$$M|N; \nu, m\rangle_{\rm JM} = m|N; \nu, m\rangle_{\rm JM} \tag{21}$$

$$m = m_a - m_b \in \{-N+|\nu|, -N+|\nu|+2, \ldots, N-|\nu|\} \tag{22}$$

for a fixed value of ν. These states have total mode number $n \stackrel{\rm def}{=} N + \nu \in \{0, 1, \ldots, 2N\}$ and energy $N + \nu + 1$. In figure 1 we arrange these states in a rhombus pattern, the same as in part I for the mode and angular momentum states of the finite Cartesian oscillator.

3.3. States of definite radius and angular momentum

The oscillator model can be Cartesian or radial, depending on our choice of the eigenbasis associated with operators of position. In the pattern below, we characterize the finite radial oscillator model by the subalgebra $so(4) \supset so(3)_{\rm R} = \text{span}\{R_1, R_2, R_3\}$,

$$\begin{array}{|c|c|c|}\hline S_3 & -S_2 & S_1 \\ \hline & R_1 & R_2 \\ \cline{2-3} & & R_3 \\ \cline{3-3}\end{array} \quad = \quad \begin{array}{|c|c|c|}\hline J & P_x & P_y \\ \hline & Q_x & Q_y \\ \cline{2-3} & & M \\ \cline{3-3}\end{array} \quad = \quad \begin{array}{|c|c|c|}\hline L_3 & -L_2 & K_1 \\ \hline & L_1 & K_2 \\ \cline{2-3} & & K_3 \\ \cline{3-3}\end{array} \tag{23}$$

Also, we point out the canonical Gel'fand–Tsetlin (GT) chain $so(4) \supset so(3)_{\rm GT} = \text{span}\{L_1, L_2, L_3\}$. These sets of generators have similar commutation relations:

$$[R_j, R_k] = \mathrm{i}\epsilon_{jkl}R_l \qquad [R_j, S_k] = \mathrm{i}\epsilon_{jkl}S_l \qquad [S_j, S_k] = \mathrm{i}\epsilon_{jkl}R_l \tag{24}$$

$$[L_j, L_k] = \mathrm{i}\epsilon_{jkl}L_l \qquad [L_j, K_k] = \mathrm{i}\epsilon_{jkl}K_l \qquad [K_j, K_k] = \mathrm{i}\epsilon_{jkl}L_l. \tag{25}$$

Because $\vec{L} = \vec{J}^{(a)} + \vec{J}^{(b)}$, the canonical chain conforms to the direct sum decomposition (14), and this implies that the irreps ℓ of $so(3)_{\rm GT}$ contained in the irrep N of $so(4)$ are those obtained from the *coupling* of two angular momenta $j = \frac{1}{2}N$ to a total angular momentum $\ell \in \{0, 1, \ldots, N\}$, with no degeneracy. This is true of any other subalgebra

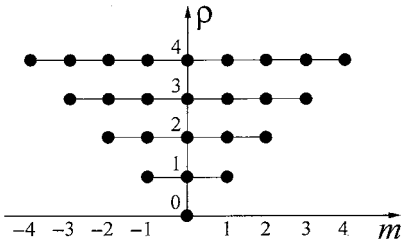

Figure 2. States $|N;\rho,m\rangle_{\rm R}$ of the two-dimensional finite oscillator, classified by angular momentum m and radius $|m| \leqslant \rho \leqslant N$. For $N = 4$ there also are 25 states.

reduction obtained by an $SO(4)$ rotation, in particular of the object of our concern: the radial subalgebra chain $so(4) \supset so(3)_{\rm R} \supset so(2)_{\rm M}$, where

$$(\vec{R})^2 \stackrel{\rm def}{=} R_1^2 + R_2^2 + R_3^2 \quad \text{spectrum:} \quad \rho(\rho+1) \quad \rho \in \{0, 1, \ldots, N\} \tag{26}$$

$$\text{and in each irrep } \rho,\ R_3 \quad \text{spectrum:} \quad m \in \{-\rho, -\rho+1, \ldots, \rho\}. \tag{27}$$

To check, we count $\sum_{\rho=0}^{N}(2\rho+1) = (N+1)^2$ independent states, matching the dimension of the $so(4)$ irrep space $N = 2j$. The $so(4)$ oscillator eigenstates of $(\vec{R})^2$ and R_3 will be denoted by $|N;\rho,m\rangle_{\rm R}$. In figure 2 we show these states rearranged with respect to the radius and angular momentum values.

4. The Clebsch–Gordan (Hahn) wavefunctions

We now build the overlap functions between the mode basis (19)–(22) and the radial basis of (26) and (27) for each allowed angular momentum. This is technically easiest in the canonical GT basis, denoted by

$$\vec{L}^2\,|N;\ell,\mu\rangle_{\rm GT} = (\vec{J}^{(a)} + \vec{J}^{(b)})^2\ |N;\ell,\mu\rangle_{\rm GT} = \ell(\ell+1)\ |N;\ell,\mu\rangle_{\rm GT} \tag{28}$$

$$L_3\ |N;\ell,\mu\rangle_{\rm GT} = (J_3^{(a)} + J_3^{(b)})\ \ |N;\ell,\mu\rangle_{\rm GT} = \mu\ |N;\ell,\mu\rangle_{\rm GT} \tag{29}$$

where naturally $\ell|_0^N$ and $\mu|_{-\ell}^{\ell}$. The overlaps between the JM and GT kets are therefore the well-known $so(3)$ Clebsch–Gordan coefficients [7, 9]. Using two convenient notations, we write

$$C^{j,j,\ell}_{m_a,m_b,\mu} = {}_{\rm GT}\langle 2j;\ell,\mu|2j;m_a{+}m_b, m_a{-}m_b\rangle_{\rm JM} \tag{30}$$

$$C^{\frac{1}{2}N,\frac{1}{2}N,\ell}_{\frac{1}{2}(\nu+m),\frac{1}{2}(\nu-m),\mu} = {}_{\rm GT}\langle N;\ell,\mu|N;\nu,m\rangle_{\rm JM}. \tag{31}$$

It should be noted that the standard form of the Clebsch–Gordan coefficients entails a phase and sign convention. Most recurrence analyses of the $so(3) \supset so(2)$ chain start with the *highest* state of the subalgebra, and not the lowest, which is the ground state here.

We must now relate the GT subalgebra chain to the chain containing the radial position subalgebra (26) and (27). This can be achieved by exchanging indices $1 \leftrightarrow 4$ and $2 \leftrightarrow 3$ in the pattern (23) by means of the $SO(4)$ transformation

$$T(\chi) \stackrel{\rm def}{=} {\rm e}^{-{\rm i}\chi(\Lambda_{2,3}-\Lambda_{1,4})} = {\rm e}^{-2{\rm i}\chi J_1^{(b)}}. \tag{32}$$

For $\chi = \pm\frac{1}{2}\pi$, and using a self-evident notation, its action on the set of $so(4)$ generators is

$$T(\tfrac{1}{2}\pi)\begin{pmatrix} L_1, L_2, L_3 \\ K_1, K_2, K_3 \end{pmatrix} T(\tfrac{1}{2}\pi)^{-1} = \begin{pmatrix} L_1, K_2, K_3 \\ K_1, L_2, L_3 \end{pmatrix} = \begin{pmatrix} R_1, R_2, R_3 \\ S_1, S_2, S_3 \end{pmatrix} \tag{33}$$

$$T(\tfrac{1}{2}\pi)\begin{pmatrix} J_1^{(a)}, J_2^{(a)}, J_3^{(a)} \\ J_1^{(b)}, J_2^{(b)}, J_3^{(b)} \end{pmatrix} T(\tfrac{1}{2}\pi)^{-1} = \begin{pmatrix} J_1^{(a)}, J_2^{(a)}, J_3^{(a)} \\ J_1^{(b)}, -J_2^{(b)}, -J_3^{(b)} \end{pmatrix}. \tag{34}$$

On the GT and mode bases, the action of $T(\frac{1}{2}\pi)$ is therefore

$$T(\tfrac{1}{2}\pi)\ |N;\ell,\mu\rangle_{\rm GT} = |N;\ell,\mu\rangle_{\rm R} \qquad T(\tfrac{1}{2}\pi)\ |N;\nu,m\rangle_{\rm JM} = |N;m,\nu\rangle_{\rm JM}. \tag{35}$$

Using as before $N = 2j$, $\nu = m_a + m_b$ and $m = m_a - m_b$, the overlap between the R and JM bases is

$$(-1)^{\rho}\Phi^{(N)}_{\nu,m}(\rho) \stackrel{\rm def}{=} {}_{\rm R}\langle N;\rho,m|N;m_a+m_b,m_a-m_b\rangle_{\rm JM} \tag{36}$$

$$= {}_{\rm GT}\langle N;\rho,m|N;m_a-m_b,m_a+m_b\rangle_{\rm JM} \tag{37}$$

$$= C^{j,j,\rho}_{m_a,-m_b,m} = C^{j,j,\rho}_{\frac{1}{2}(m+\nu),\frac{1}{2}(m-\nu),m} \tag{38}$$

where $|m| \leqslant \rho \leqslant N$ are integers and

$$\text{for}\quad \nu\,|^{N}_{-N}\ \text{fixed}\quad m \in \{-N+|\nu|,-N+|\nu|+2,\ldots,N-|\nu|\} \tag{39}$$

$$\text{for}\quad m|^{N}_{-N}\ \text{fixed}\quad \nu \in \{-N+|m|,-N+|m|+2,\ldots,N-|m|\}. \tag{40}$$

The explicit form of the finite radial oscillator states can be written using standard expressions in terms of hypergeometric ${}_3F_2$ functions:

$$\Phi^{(N)}_{\nu,m}(\rho) = (-1)^{\frac{1}{2}N-m_a+\rho}\,\frac{N!}{\Gamma(m+1)} \times\sqrt{\frac{(2\rho+1)}{\Gamma(N-\rho+1)\,\Gamma(N+\rho+2)}\,\frac{(\rho+m)!}{(\rho-m)!}\,\frac{(\frac{1}{2}N+m_b)!\,(\frac{1}{2}N-m_b)!}{(\frac{1}{2}N+m_a)!\,(\frac{1}{2}N-m_a)!}} \times{}_3F_2\left(\begin{matrix}-\rho,\ \rho+1,\ -\frac{1}{2}N+m_a\\ m+1,\ -N\end{matrix}\,\middle|\,1\right) \tag{41}$$

$$= (-1)^{\rho+2m_a}\,\Phi^{(N)}_{\nu,-m}(\rho) \tag{42}$$

with $m_a = \frac{1}{2}(\nu+m)$, $m_b = \frac{1}{2}(\nu-m)$, and the parameter ranges in equations (39) and (40).

In figure 3 we show the linear combinations of finite oscillator states that map between the mode and radius bases, for fixed angular momentum m. Their overlap yields the real radial wavefunctions $\Phi^{(N)}_{\nu,m}(\rho)$ in (36)–(41) shown in figures 4. We plot the four lowest, the middle and the four highest energy states. The first ($\nu \approx -N$) resemble the ordinary quantum radial wavefunctions multiplied by the root of the radial measure $\sqrt{r}$ (this does *not* mean a singularity at $\rho = 0$). The last ($\nu \approx N$) have the same appearance as the previous ones, but alternate sign between every two points; this is due to the sign identity between Clebsch–Gordan coefficients $C^{j,j,\rho}_{m_a,m_b,m} = (-1)^{\rho}C^{j,j,\rho}_{m_b,m_a,m}$, which relates the two wavefunctions with $\pm\nu$. The middle radial states $\nu = 0$ resemble the right half of the middle 1D oscillator Kravchuk function in figure 1 of part I [1] and highlight the fact that the overlap functions exist only for radii $\rho \geqslant |m|$.

As we noted after (30) and (31), the Clebsch–Gordan coefficients were originally built to minimize changes of sign for m_a and m_b near to j. The finite radial wavefunctions we defined in (36) require the sign $(-1)^{\rho}$ to avoid oscillations near the ground state. This is confirmed by a new limit relation (to be proven in detail elsewhere) for $\rho = r\sqrt{N}$, $N \to \infty$, with $n = j+m_a$ and $m = m_a - m_b$ finite:

$$\lim_{N\to\infty} N^{\frac{1}{4}}\,(-1)^{\rho}C^{j,j,\rho}_{m_a,-m_b,m} = (-1)^{N-n}\sqrt{\frac{2\,n!}{(n+|m|)!}}\ r^{|m|+\frac{1}{2}}\,{\rm e}^{-\frac{1}{2}r^2}\,L^{|m|}_n(r^2). \tag{43}$$

The extra factor of $r^{\frac{1}{2}}$ corresponds to the square root of the radial integration measure.

The finite radial oscillator wavefunctions are thus Clebsch–Gordan coefficients of $so(3)$. We recall here a similar case: the Pöschl–Teller potential also has wavefunctions that are Clebsch–Gordan coefficients, but of $so(2,1)$—with its very structured set of discrete and continuous irrep series [12, 13]. In $so(4)$ all indices and arguments are discrete, but moreover,

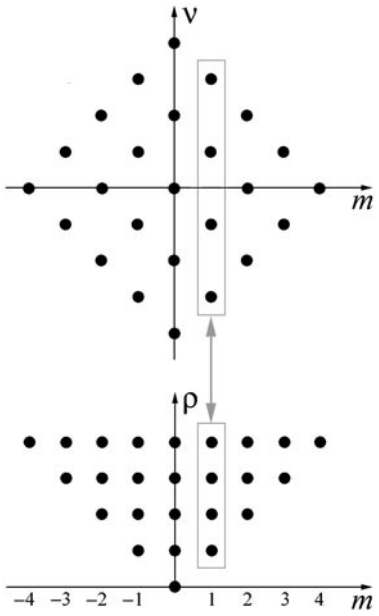

Figure 3. The map between states of the same angular momentum m in the two previous figures is indicated by the up–down arrow $\updownarrow$. States in the thin rectangles are linear combinations of each other; states of different m's are orthogonal. The overlaps are the finite radial oscillator wavefunctions $\Phi^{(N)}_{\nu,m}(\rho)$ given with $su(2)$ Clebsch–Gordan coefficients.

as was the case with the Kravchuk [14] and Meixner [15,16] oscillators, the wavefunctions turn out to have a polynomial factor that allows a special analytic continuation in one variable. In the Kravchuk and Meixner cases this variable is the position, so finite systems can be thought of having a 'continuous' position coordinate. The existence of this analytic continuation is important because it permits the dynamical algebra to be realized by *difference operators* that bind any three points of the position variable separated by units, within (and one unit outside) the interval. Hence there exists a Schrödinger difference equation to rule over finite systems [2,3,16].

It is very satisfying that a discrete polynomial family exists for the finite radial oscillator (and indeed for $so(3)$ Clebsch–Gordan coefficients): *dual Hahn polynomials* [17–20]. These polynomials are defined by the ${}_3F_2$ hypergeometric function of unit argument

$$R_n\big(\rho(\rho+1);m,-m,N\big) \stackrel{\text{def}}{=} {}_3F_2\left(\left.\begin{matrix}-n,\ -\rho,\ \rho+1\\ m+1,\ -N\end{matrix}\right|1\right) \tag{44}$$

for degree n in $\rho(\rho+1)$. Due to the polynomial, the finite radial wavefunctions can be analytically continued in the radius ρ; the square root factor is analytic in ρ on the open interval $\max(|m|-1,-\frac{1}{2})<\rho<N+1$, with branch zeros at the endpoints.

5. Discrete radii and discrete angles

For fixed angular momentum m, there are $N-|m|$ independent functions (41) distinguished by $\nu\in\{-N+|m|,-N+|m|+2,\ldots,N-|m|\}$ which are functions of the same number of radii $\rho|_{|m|}^{N}$. For each angular momentum, the functions are real and form an orthonormal and complete set:

$$\sum_{\nu=-N+|m|:\,(+2)}^{N-|m|}\Phi^{(N)}_{\nu,m}(\rho)\,\Phi^{(N)}_{\nu,m}(\rho')=\delta_{\rho,\rho'}\qquad\sum_{\rho=|m|}^{N}\Phi^{(N)}_{\nu,m}(\rho)\,\Phi^{(N)}_{\nu',m}(\rho)=\delta_{\nu,\nu'} \tag{45}$$

where the sum notation ': (+2)' is meant to remind us that the values of ν are spaced by 2. These relations agree, of course, with the known bilinear sums of Clebsch–Gordan

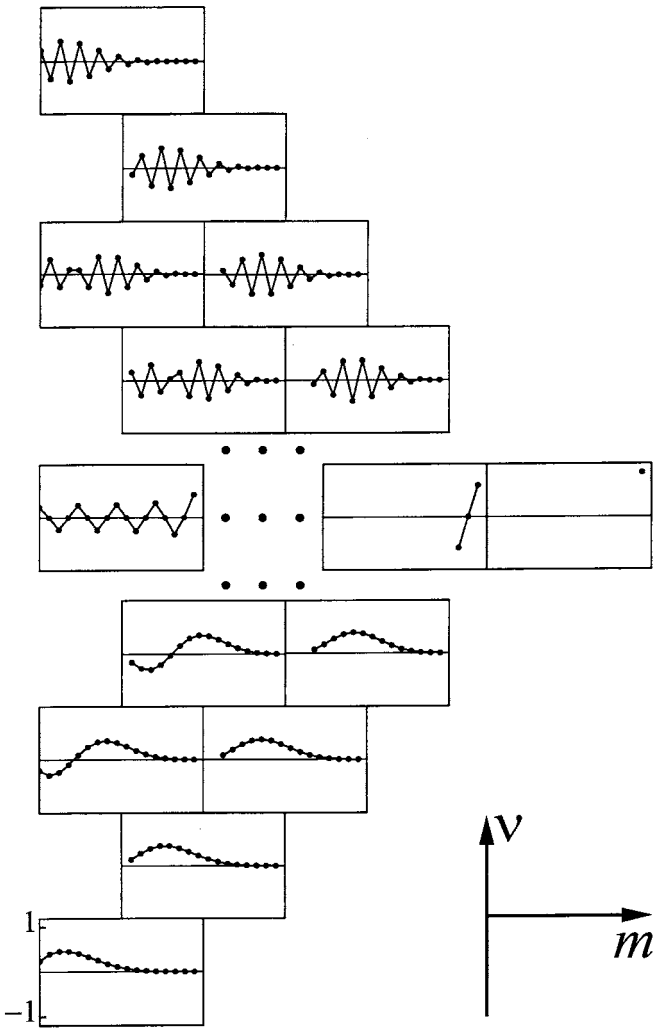

Figure 4. Wavefunctions $\Phi^{(N)}_{\nu,m}(\rho)$ of the two-dimensional finite radial oscillator for $N = 16$ ($j = 8$). The individual graphs are arranged from bottom to top by mode (∼energy) $j + \nu = 0, 1, 2, 3, \ldots, 8, \ldots, 13, 14, 15, 16$ and from left to right by columns of angular momentum $m = 0, 1, 2, 3, \ldots, 7, 8$. The functions are defined in the ranges $|m| \leqslant \rho \leqslant N$ of the radius. For visibility, we interpolate linearly the values of the function between integer radii; they are ($(-1)^{\rho}$ times) the $su(2)$ Clebsch–Gordan coefficients. The lower states resemble ($\sqrt{r}$ times) the Laguerre wavefunctions of the 'continuous' quantum oscillator; these have an $|m|$-fold zero at the origin.

coefficients ([9], section 8.7.2).

On the other hand, for a fixed value of the radius $\rho|_0^N$, the spectrum (39) of angular momenta is the set of $2\rho + 1$ values $m \in \{-\rho, -\rho + 1, \ldots, \rho\}$. Because of (21) and (27), for each ρ the set of angular momentum states will be orthogonal and complete:

$$ {}_{\mathrm{R}}\langle N; \rho, m | N; \rho, m' \rangle_{\mathrm{R}} = \delta_{m,m'} \qquad \sum_{m=-\rho}^{\rho} |N; \rho, m\rangle_{\mathrm{RR}}\langle N; \rho, m| = \hat{1}_{\rho} \tag{46} $$

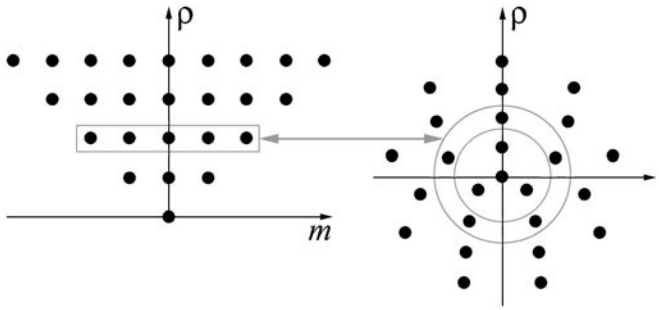

Figure 5. The states $|N;\rho,m\rangle_{\mathrm{R}}$ (left, as in figure 2), indicated by a thin rectangle for definite radius ρ, under the discrete Fourier transform map ($\leftrightarrow$) on the points on the circle indicated by thin lines, of radius ρ in the array of Kronecker position states $|N;\rho,\theta_k\rangle_\circ$ (right).

where $\hat{1}_\rho$ is the unit operator in each irrep space ρ, and the inner product is defined abstractly (thus far). Clearly, at a fixed radius, the natural Hilbert space is that of functions on the circle or, since there are a finite number of m's, $2\rho+1$ points equidistant on a circle obtained through the discrete Fourier transform. Thus, for each radius ρ we introduce the (discrete) angles (also used as *labels*)

$$\theta_k = \frac{2\pi k}{2\rho+1} \qquad k \in \{-\rho, -\rho+1, \ldots, \rho\} \tag{47}$$

to define new *radius-and-angle* kets by the linear combinations

$$|N;\rho,\theta_k\rangle_\circ \stackrel{\mathrm{def}}{=} \frac{1}{\sqrt{2\rho+1}} \sum_{m=-\rho}^{\rho} \mathrm{e}^{\mathrm{i}m\theta_k}\, |N;\rho,m\rangle_{\mathrm{R}} \tag{48}$$

$$|N;\rho,m\rangle_{\mathrm{R}} = \frac{1}{\sqrt{2\rho+1}} \sum_{k=-\rho}^{\rho} \mathrm{e}^{-\mathrm{i}m\theta_k}\, |N;\rho,\theta_k\rangle_\circ \tag{49}$$

that are a Kronecker basis of states for the circle of radius ρ. The overlaps are ${}_\circ\langle N;\rho,\theta_k|N;\rho,m\rangle_{\mathrm{R}} = \mathrm{e}^{-\mathrm{i}m\theta_k}/\sqrt{2\rho+1}$. The radius-and-angle kets are cyclic functions of θ_k modulo 2π (or of k modulo N), so we interpret θ straightforwardly as the angular coordinate in the point array shown in figure 5.

At the centre of the array, $\rho = 0$, there is only one state $m = 0$ and one angle θ_0 (which is irrelevant). The space is one dimensional and its only state is $|N;0,\theta_0\rangle_\circ = |N;0,0\rangle_{\mathrm{R}}$. On the first circle, of radius $\rho = 1$, there are three states, $m = 0$ and $m = \pm 1$. Correspondingly, as shown in figure 5, there are three points on the circle, of angles $\theta_0 = 0$ and $\theta_{\pm 1} = \pm\frac{2}{3}\pi$. (We do have the freedom to rotate this circle by a 'starting angle' $\theta_k \mapsto \theta_k + \bar{\theta}(\rho)$ (which may be different for each radius ρ), introducing the corresponding phase changes in (48) and (49) but here this does not seem useful enough to carry further.) On the following circles, of radii $\rho = 2, 3, \ldots$, there will be $2\rho + 1$ points, sensors or pixels around each circle. Finally, there is a maximal circle $\rho = N$ with the maximal number $2N + 1$ of angular momentum states and points around that circle. There is nothing beyond.

When the discrete surface element in polar coordinates is measured by $\Delta^2\boldsymbol{r} \stackrel{\mathrm{def}}{=} \rho\,\Delta\rho\,\Delta\theta_k$, the array of figure 5, having $\Delta\rho = 1$ and $\Delta\theta_k = \theta_k - \theta_{k-1} = 2\pi/(2\rho+1)$, will exhibit a 'density of points' $\pi\rho/(\rho+\frac{1}{2})$; as ρ grows, this density rather quickly becomes π. In figure 6 we show the points on which a radial/angular finite wavefield is defined for a moderately large number of circles N. A finite wavefield $\psi^{(N)}$ is determined by a set of complex values on the

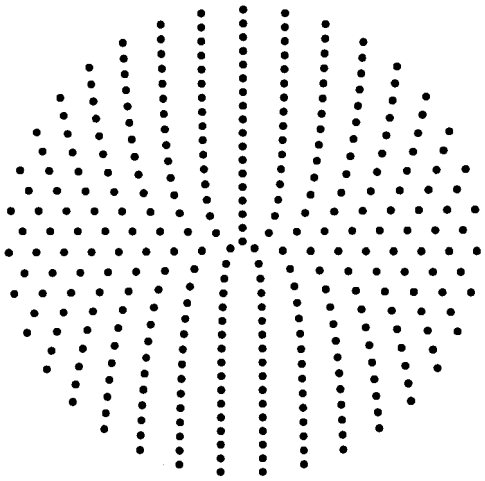

Figure 6. Position space for a finite radial oscillator with $N = 40$ circles (plus the centre). Notice the 'homogeneous grey' density of points.

array of points with radius and angle $\psi_{\circ}^{(N)}(\rho, \theta_k)$ given by the overlap

$$\psi_{\circ}^{(N)}(\rho, \theta_k) = {}_{\circ}\langle N; \rho, \theta_k | N; \psi\rangle \tag{50}$$

$$= \sum_{m=-\rho}^{\rho} {}_{\circ}\langle N; \rho, \theta_k | N; \rho, m\rangle_{\mathrm{RR}}\langle N; \rho, m | N; \psi\rangle \tag{51}$$

$$= \frac{1}{\sqrt{2\rho+1}} \sum_{m=-\rho}^{\rho} \mathrm{e}^{-\mathrm{i}m\theta_k}\, \psi_m^{(N)}(\rho) \tag{52}$$

$$= \frac{(-1)^{\rho}}{\sqrt{2\rho+1}} \sum_{m=-\rho}^{\rho} \mathrm{e}^{-\mathrm{i}m\theta_k} \sum_{\nu=-N+|m|:\,(+2)}^{N-|m|} C^{\frac{1}{2}N,\frac{1}{2}N,\rho}_{\frac{1}{2}(m+\nu),\frac{1}{2}(m-\nu),m}\, \psi_{\nu,m}^{(N)}. \tag{53}$$

The same wavefield is determined by the set of values $\psi^{(N)}(\rho, m)$ in the R basis of radius and angular momentum, and by $\psi_{\nu,m}^{(N)}$ in the JM basis of mode and angular momentum. Between them, the Parseval relation holds:

$$(\psi^{(N)}, \phi^{(N)}) \stackrel{\mathrm{def}}{=} \sum_{\rho=0}^{N} \sum_{k=-\rho}^{\rho} \psi_{\circ}^{(N)}(\rho, \theta_k)^*\, \phi_{\circ}^{(N)}(\rho, \theta_k)$$

$$= \sum_{\nu=-N}^{N} \sum_{m=-N+|\nu|:\,(+2)}^{N-|\nu|} \psi^{(N)}(\nu, m)^*\, \phi^{(N)}(\nu, m). \tag{54}$$

6. Finite fractional Hankel–Hahn transforms

The one-dimensional fractional Fourier integral transform of power α (modulo 4) is generated by the oscillator number operator $H - \frac{1}{2}$, whose action on the wavefunctions of mode ν is to multiply them by the phases $\mathrm{e}^{-\mathrm{i}\frac{1}{2}\pi\nu\alpha}$; this is the $U(1)$ Fourier symmetry group of the oscillator. Correspondingly, in the one-dimensional finite oscillator model of $N+1$ points [3], the same argument leads to the fractional Fourier–Kravchuk transform, so called because Kravchuk functions are involved; the kernel turns out to be an $SU(2)$ Wigner 'little d' function $d^{\frac{1}{2}N}_{q,q'}(\frac{1}{2}\pi\alpha)$ [5] which, when $N \to \infty$, becomes the ordinary Fourier transform [21]. In yet another model, the discrete (but infinite) radial oscillator based on $so(2, 1)$ [16] contains a

transform that was called Hankel–Meixner, because Meixner functions appear through the Bargmann d-functions $d^k_{m,r}(\zeta)$ of $so(2,1)$ [22] which, when $N \to \infty$, becomes the ordinary fractional Hankel transform [23]. In this paper we are introducing the fractional Hankel–Hahn transform which is contained in the $so(4)$ finite oscillator model.

In two dimensions, the symmetry group of the quantum oscillator is the group of $U(2)$ Fourier transforms [24]. The integral kernel of the $U(1)$ centre of this group can be decomposed into a series of Hankel transforms of integer order m with discrete Fourier transforms for the angle. In each angular momentum subspace $\pm m$, the integral transform kernel is a Bessel function of the first kind, $J_m(k^2 r' r)$, in the radial coordinate $r|_0^\infty$. In the two-dimensional *finite* oscillator model, the number operator is $H - 1 = J + E_J$, $E_J = j\hat{1}$, as in (7). The following are the *fractional Fourier operators*:

$$\mathcal{F}^\alpha = \exp\left(-\mathrm{i}\tfrac{1}{2}\pi\alpha(J + E_J)\right) \tag{55}$$

of power α mod 4 and angle $\frac{1}{2}\pi\alpha$. In the basis of the mode-angular momentum kets of the irrep $N = 2j$ of $so(4)$, $|N;\nu,m\rangle_{\mathrm{JM}}$ in (19)–(22), the Fourier operators (55) are represented by the diagonal matrices

$$F^\alpha_{\mathrm{JM}}(\nu,m;\nu',m') = {}_{\mathrm{JM}}\langle N;\nu,m|\mathcal{F}^\alpha|N;\nu',m'\rangle_{\mathrm{JM}} = \delta_{\nu,\nu'}\,\delta_{m,m'}\,\mathrm{e}^{-\mathrm{i}\frac{1}{2}\pi(\nu+j)\alpha} \tag{56}$$

while in the basis $|N;\rho,m\rangle_{\mathrm{R}}$, they are represented by matrices obtained from the overlaps (36)–(40)

$$F^{(N,\alpha)}_{\mathrm{R}}(\rho,m;\rho',m') = {}_{\mathrm{R}}\langle N;\rho,m|\mathcal{F}^\alpha|N;\rho',m'\rangle_{\mathrm{R}} = \delta_{m,m'}\,H^{(N,\alpha)}_m(\rho,\rho'). \tag{57}$$

The latter matrices are block-diagonal in m, because the orbital angular momentum M commutes with the generator of the central Fourier transforms. Using (36)–(40), we find the $(N - |m|) \times (N - |m|)$ submatrices, with rows and columns numbered by $\rho, \rho' \in \{|m|, |m|+1, \ldots, N\}$, given by

$$H^{(N,\alpha)}_m(\rho,\rho') = {}_{\mathrm{R}}\langle N;\rho,m|\mathcal{F}^\alpha|N;\rho',m\rangle_{\mathrm{R}} \tag{58}$$

$$= \sum_{\nu=-N+|m|:\,(+2)}^{N-|m|} {}_{\mathrm{R}}\langle N;\rho,m|N;\nu,m\rangle_{\mathrm{JM}}\,\mathrm{e}^{-\mathrm{i}\frac{1}{2}\pi(\nu+j)\alpha}\,{}_{\mathrm{R}}\langle N;\nu,m|N;\rho',m\rangle_{\mathrm{R}} \tag{59}$$

$$= \sum_{\nu=-N+|m|:\,(+2)}^{N-|m|} (-1)^{\rho+\rho'}\,C^{j,j,\rho}_{\frac{1}{2}(m+\nu),\frac{1}{2}(m-\nu),m}\,\mathrm{e}^{-\mathrm{i}\frac{1}{2}\pi(\nu+j)\alpha}\,C^{j,j,\rho'}_{\frac{1}{2}(m+\nu),\frac{1}{2}(m-\nu),m}. \tag{60}$$

The Hankel–Hahn transforms are finite N approximations to the Hankel integral transforms. Indeed, we have shown (to be detailed elsewhere) that, for $N \to \infty$, the summation kernel (60) of the former becomes the integral kernel of the latter. When $\rho = r\sqrt{N}$ and $\rho' = r'\sqrt{N}$, while mode number $n = \nu + j$ and angular momentum m remain finite, we can use (43) to prove (with $m_a = \frac{1}{2}(\nu+m)$, $m_b = \frac{1}{2}(\nu-m)$ and $N = 2j$ as before)

$$\lim_{N\to\infty} H^{(N,\alpha)}_m(\rho,\rho') = \sum_{n=0}^{\infty}(-1)^n\frac{2\,n!}{(n+|m|)!}\,(r\,r')^{|m|+\frac{1}{2}}\,\mathrm{e}^{-\frac{1}{2}(r^2+r'^2)}\,L^{|m|}_n(r^2)\,L^{|m|}_n(r'^2) \tag{61}$$

$$= \frac{(-\mathrm{i})^m\,\mathrm{e}^{\mathrm{i}\pi m\alpha}}{\sin\frac{1}{2}\pi m\alpha}\exp\left[\mathrm{i}\frac{1}{2}(r^2+r'^2)\cot\frac{1}{2}\pi\alpha\right]\sqrt{r\,r'}\,J_m\left(\frac{r\,r'}{\sin\frac{1}{2}\pi\alpha}\right). \tag{62}$$

For a fixed angular momentum m, the functions $\psi^{(N)}_m(\rho) = {}_{\mathrm{R}}\langle N;\rho,m|\psi\rangle$ of radii $|m| \leqslant \rho \leqslant N$ will transform under the *fractional Hankel–Hahn transform* with the kernel (60)

$$\mathcal{F}^\alpha : \psi^{(\mathrm{N})}_m(\rho) = \sum_{\rho'=|m|}^{N} H^{(N,\alpha)}_m(\rho,\rho')\,\psi^{(\mathrm{N})}_m(\rho'). \tag{63}$$

The label m is unaffected by $\mathcal{F}^\alpha$ because J and M commute. In the radius and angle basis (48), however, we compute

$$\mathcal{F}^\alpha : \psi^{(N)}(\rho, \theta_k) = \sum_{m=-\rho}^{\rho} \sum_{\rho'=|m|}^{N} \sum_{k=-\rho'}^{\rho'} \frac{\mathrm{e}^{-\mathrm{i}m(\theta_k - \theta_{k'})}}{\sqrt{(2\rho+1)(2\rho'+1)}} H_m^{(N,\alpha)}(\rho, \rho')\, \psi^{(N)}(\rho', \theta_{k'}). \tag{64}$$

Only in the limit $N \to \infty$, when the sum over m becomes unbounded, will the transform leave θ unaffected, as it is under the Hankel integral transform.

We call attention to the fact that, for $|m| > 0$, the Hankel–Hahn transforms are defined only on an annulus of radii between $|m|$ and N. It is the suggested counterpart of a property in the ordinary Hankel transform: $J_m(r'r)$ has an $|m|$-fold zero at the origin. The group theoretical meaning of the fractional Hankel–Hahn matrices, which generalizes that of the Fourier–Kravchuk matrices, can be seen by writing (58) in terms of the $so(4)$ generators and recalling $T(\chi)$ from (32)–(35), namely

$$H_m^{(N,\alpha)}(\rho, \rho') = {}_{\mathrm{GT}}\langle N; \rho, m | T(\tfrac{1}{2}\pi)^{-1}\, \mathrm{e}^{-\mathrm{i}\frac{1}{2}\pi\alpha\Lambda_{1,2}}\, T(\tfrac{1}{2}\pi)\, |N; \rho', m\rangle_{\mathrm{GT}} \tag{65}$$

$$= {}_{\mathrm{GT}}\langle N; \rho, m | \mathrm{e}^{-\mathrm{i}\frac{1}{2}\pi\alpha\Lambda_{3,4}}\, |N; \rho', m\rangle_{\mathrm{GT}} \stackrel{\mathrm{def}}{=} d^{N,0}_{\rho,m,\rho'}(\tfrac{1}{2}\pi\alpha). \tag{66}$$

Generally, $d^{N_1,N_2}_{\ell,m,\ell'}(\theta)$ are the $SO(4)$ analogue of the $SO(3)$ Wigner little d's [25]: the matrix elements of the 'last' rotation angle (generated by the 'lowest' generator in the pattern (11)) within the generic $so(4)$ representation (N_1, N_2), where $N_1 \geqslant \ell, \ell' \geqslant |N_2|$ and $\ell, \ell' \geqslant |m|$. For $so(D)$ see [26].

7. Contraction to the continuum

For a finite oscillator model to be adequate, it should display a well-defined contraction limit to the ordinary quantum oscillator when $2j = N \to \infty$, in the two dimensions of our concern. The contraction will be made here for the generators 'in the weak sense', glossing over the proper definition of the limit for Hilbert spaces of increasing and infinite dimension recently validated by Barker [27].

Consider the following change of generator basis that scales the six generators of $so(4)$ and the irrep operator $E_J = j\hat{1}$ in (5):

$$\begin{aligned} \vec{Q}^{(j)} &\stackrel{\mathrm{def}}{=} \vec{Q}/\sqrt{j} \qquad & J^{(j)} &\stackrel{\mathrm{def}}{=} J + (1 + j^{-1})\, E_J \\ \vec{P}^{(j)} &\stackrel{\mathrm{def}}{=} \vec{P}/\sqrt{j} \qquad & M^{(j)} &\stackrel{\mathrm{def}}{=} M \end{aligned} \tag{67}$$

and the Hamiltonian

$$H^{(j)} = J^{(j)} + (j+1)\hat{1} = H. \tag{68}$$

As $j \to \infty$, the eigenvalues of position shrink equidistantly by $j^{-1/2}$ in the growing interval $[-\sqrt{j}, \sqrt{j}]$, while those of energy and angular momentum, H and M, retain the spacing. The commutators of the (j) generators are evidently determined by those of the original generators. The two Hamilton equations (1) and the defining properties of angular momentum (2) are independent of j. On the other hand, the nonstandard commutators between position and momentum and between the x and y components of vectors, equations (12), (13), become the standard ones:

$$\left.\begin{aligned} [Q^{(\phi)}, P^{(\phi)}] &= \mathrm{i}\, J \\ [Q^{(\phi)}, P^{(\phi+\frac{1}{2}\pi)}] &= 0 \\ [R_x^{(\theta)}, R_y^{(\theta)}] &= \mathrm{i}M \end{aligned}\right\} \Rightarrow \begin{cases} [Q_x^{(\infty)}, P_x^{(\infty)}] = \mathrm{i}\hat{1} = [Q_y^{(\infty)}, P_y^{(\infty)}] \\ [Q_x^{(\infty)}, P_y^{(\infty)}] = 0 = [Q_y^{(\infty)}, P_x^{(\infty)}] \\ [Q_x^{(\infty)}, Q_y^{(\infty)}] = 0 = [P_y^{(\infty)}, P_x^{(\infty)}]. \end{cases} \tag{69}$$

The contracted algebra has seven generators: position, momentum and the unit form the Heisenberg–Weyl five-generator algebra $W_2 = \mathrm{span}\{\vec{Q}, \vec{P}, \hat{1}\}$; the Hamiltonian and angular momentum are given by the limit of the two Casimir operators (16) and (17), which imply the 'ordinary' quantum-mechanical forms

$$H^{(\infty)} = \tfrac{1}{2}\big((\vec{P}^{(\infty)})^2 + (\vec{Q}^{(\infty)})^2\big) \qquad M^{(\infty)} = Q_x^{(\infty)} P_y^{(\infty)} - Q_y^{(\infty)} P_x^{(\infty)}. \quad (70)$$

8. Conclusions

In parts I and II of this series on the finite oscillator in two dimensions, we have explored $so(4)$ as the dynamical algebra for the Cartesian and radial models, within symmetric representations of dimension $(N+1)^2$. The difference between the two models is the asignment of observables to generators: in the Cartesian model, the x and y components of position commute, while in the radial model their commutator is angular momentum; and it is the spectrum of the Casimir operator of that subalgebra which provides the range of radii. The angles are here ancillary to the spectrum of the angular momentum operator.

The discretization of physical and information systems, performed in such a way that it respects the Hamiltonian structure and phase-space dynamics, is important in several branches of science. The harmonic oscillator is paradigmatic of theoretical physics, as the waveguide is in optics and image processing. All entail the fractional Fourier transform, one of whose current areas of application is in signal analysis [28, 29]. The issue of its discretization cannot be said to be satisfactorily solved until a set of desirable factors is agreed upon. The existence of coherent states [30] in finite systems as in their continuous limit seems important to us. Such states are guaranteed to exist [5] within any compact Lie-theoretic model when the Hamiltonian is a linear function of the group generators; they will satisfy a 'Schrödinger' second-order *difference* equation. Nonlinear systems such as the (quadratic) Kerr effect [31] will present periodic phenomena (revivals of cat states) that are generic and stable under contraction. The known mathematical results of the theory of discrete polynomials (Kravchuk, Meixner, Pollaczek, Hahn, etc) and of angular momentum theory (Wigner D functions, spherical harmonics, coefficients of Clebsch–Gordan, Racah, 6- and 9-j symbols, etc) are given a new interpretation. Finite algorithms with the same unitarity properties as their continuum limits should be compared with the standard (and highly refined) numerical methods, in sonar acoustics [32] for example, to evaluate the Hankel transform on a finite polar array.

There are at least two questions to be addressed in a third paper in this series: the unitary map between the Cartesian and polar models (in image-processing terms, the transformation between a square-pixellated image and its polar pixellation) and a putative relation between rectangular screens, non-symmetric $so(4)$ representations and possible discrete elliptic coordinates. The study of higher dimensions may present the question of sampling functions on conics. Research into finite Schrödinger–Robertson uncertainty relations (which have become available recently for finite and infinite Fourier series [33,34]), and a phase-space picture based on Wigner quasiprobability distribution functions (for finite systems on compact Lie algebras see [35,36]), should provide further insights into handling sets of discrete data on systems that we usually regard as continuous.

Acknowledgments

KBW would like to acknowledge a short but particularly lucid conversation with M Moshinsky (Instituto de Física, UNAM) and the original interest in a discrete Hankel transform by

J D Secada (ICIMAF, Cuba). The authors thank the support of the Dirección General de Asuntos del Personal Académico, Universidad Nacional Autónoma de México (DGAPA–UNAM) by grant IN112300 *Optica Matemática*. GSP acknowledges the Consejo Nacional de Ciencia y Tecnología (México) for a Cátedra Patrimonial Nivel II, and Russian Foundation for Basic Research, grant RFBR N00–02–81023. LEV thanks CONACYT Graduate Scholarship no 150666.

References

[1] Atakishiyev N M, Pogosyan G S, Vicent L E and Wolf K B 2001 Finite two-dimensional oscillator: I. Cartesian model *J. Phys. A: Math. Gen.* **34** 9349–66 (preceding paper)
[2] Atakishiyev N M and Suslov S K 1991 Difference analogs of the harmonic oscillator *Theor. Math. Phys.* **85** 1055–62
[3] Atakishiyev N M and Wolf K B 1997 Fractional Fourier–Kravchuk transform *J. Opt. Soc. Am.* A **14** 1467–77
[4] Arık M, Atakishiyev N M and Wolf K B 1999 Quantum algebraic structures compatible with the harmonic oscillator Newton equation *J. Phys. A: Math. Gen.* **32** L371–6
[5] Atakishiyev N M, Vicent L E and Wolf K B 1999 Continuous versus discrete fractional Fourier transforms *J. Comput. Appl. Math.* **107** 73–95
[6] Wolf K B 1967 Dynamical groups for the point rotor and the hydrogen atom *Suppl. Nuovo Cimento* **5** 1041–50
[7] Biedenharn L C and Louck J D 1981 Angular momentum in quantum physics *Encyclopedia of Mathematics and Its Applications* ed G-C Rota (Reading, MA: Addison-Wesley)
[8] Pogosyan G S and Ter-Antonyan V M 1978 The connection between Cartesian and polar wavefunctions of a circular oscillator and the dynamical $O(3)$ symmetry *Izv. Akad. Nauk Arm. SSR Fiz.* **13** 235–7
Pogosyan G S, Smorodinsky Ya A and Ter-Antonyan V M 1981 Oscillator Wigner functions *J. Phys. A: Math. Gen.* **14** 769–76
Mardoyan L A, Pogosyan G S, Sissakian A N and Ter-Antonian V M 1985 Interbasis expansions in a circular oscillator *Nuovo Cimento* A **86** 324–36
[9] Varshalovich D A, Moskalev A N and Khersonskiĭ V K 1988 *Quantum Theory of Angular Momentum* (Singapore: World Scientific)
[10] Frank A and Van Isacker P 1998 *Algebraic Methods in Molecular and Nuclear Structure Physics* (New York: Wiley)
[11] Stone A P 1956 Some properties of Wigner coefficients and hyperspherical harmonics *Proc. Camb. Phil. Soc.* **52** 424–30
[12] Basu D and Wolf K B 1983 The Clebsch–Gordan coefficients of the three-dimensional Lorentz algebra in the parabolic basis *J. Math. Phys.* **24** 478–500
[13] Frank A and Wolf K B 1985 Lie algebras for systems with mixed spectra. The scattering Pöschl–Teller potential *J. Math. Phys.* **26** 973–85
[14] Atakishiyev N M and Wolf K B 1994 Approximation on a finite set of points through Kravchuk functions *Rev. Mex. Fís.* **40** 366–77
[15] Atakishiyev N M, Jafarov E I, Nagiyev S M and Wolf K B 1998 Meixner oscillators *Rev. Mex. Fís.* **44** 235–44
[16] Atakishiyev N M, Nagiyev Sh M, Vicent L E and Wolf K B 2000 Covariant discretization of axis-symmetric linear optical systems *J. Opt. Soc. Am.* A **17** 2301–14
[17] Hahn W 1949 Über orthogonalpolynome, die q-differenzengleichungen genügen *Math. Nachr.* **2** 4–34
[18] Erdelyi A *et al* (ed) 1953 *Higher Transcendental Functions* vol 2 (New York: McGraw-Hill) section 10.23 equation (12)
[19] Nikiforov A F, Suslov S K and Uvarov V B 1991 Classical orthogonal polynomials of a discrete variable *(Springer Series in Computational Physics)* (Heidelberg: Springer) equations (5.2.13) and (5.2.14)
[20] Koekoek R and Swarttow R F 1998 The Askey-scheme of hypergeometric orthogonal polynomials and its q-analogue *Report* No 98–17 Delft University of Technology, Delft 34
[21] Atakishiyev N M, Pogosyan G S, Vicent L E and Wolf K B Contractions of the finite oscillator submitted
[22] Bargmann V 1947 Unitary irreducible representations of the Lorentz group *Ann. Math.* **48** 568–640
[23] Namias V 1980 Fractionalization of Hankel transforms *J. Inst. Math. Appl.* **26** 187–97
[24] Simon R and Wolf K B 2000 Fractional Fourier transforms in two dimensions *J. Opt. Soc. Am.* A **17** 2368–81
[25] Biedenharn L C 1961 Wigner coefficients for the R_4 group and some applications *J. Math. Phys.* **2** 433–41
Freedman D Z and Wang J-M 1967 $O(4)$ symmetry and Regge-pole theory *Phys. Rev.* **160** 1560–71
[26] Wolf K B 1971 A recursive method for the calculation of the SO_n, $SO_{n,1}$, and ISO_n representation matrices *J. Math. Phys.* **12** 197–206

[27] Barker L 2001 Continuum quantum systems as limits of discrete quantum systems: I. State vectors *J. Funct. Anal.* at press
Barker L 2001 Continuum quantum systems as limits of discrete quantum systems: II. State functions *J. Phys. A: Math. Gen.* **34** 4673–82
Barker L 2001 Continuum quantum systems as limits of discrete quantum systems: III. Operators *J. Math. Phys.* at press
Barker L 2001 Continuum quantum systems as limits of discrete quantum systems: IV. Affine canonical transforms *Preprint* Bilkent University
[28] Ozaktas H M, Alper Kutay M and Mendlovic D 1999 Introduction to the fractional Fourier transform and its applications *Advances on Imaging and Electron Optics* vol 106 pp 239–91 ch 4
[29] Ozaktas H M, Zalevsky Z and Alper Kutay M 2000 *The Fractional Fourier Transform* (Chichester: Wiley)
[30] Perelomov A M 1986 *Generalized Coherent States and Their Applications* (Berlin: Springer)
[31] Chumakov S M, Frank A and Wolf K B 1999 Finite Kerr medium: macroscopic quantum superposition states and Wigner functions on the sphere *Phys. Rev.* A **60** 1817–23
[32] Candel S M 1981 An algorithm for the Fourier–Bessel transform, *Comput. Phys. Commun.* **23** 343
Secada J D 1999 Numerical evaluation of the Hankel transform *Comput. Phys. Commun.* **116** 278–94
[33] Opatrný T 1994 Mean value and uncertainty of optical phase—a simple mechanical analogy *J. Phys. A: Math. Gen.* **27** 7201–8
Opatrný T 1995 Number-phase uncertainty relations *J. Phys. A: Math. Gen.* **28** 6961–75
[34] Forbes G W and Alonso M A 2001 Measures of spread for periodic distributions and the associated uncertainty relations *Am. J. Phys.* **69** 340–7
Forbes G W and Alonso M A Consistent analogues of the Fourier uncertainty relations *Am. J. Phys.* **69** (9)
[35] Atakishiyev N M, Chumakov S M and Wolf K B 1998 Wigner distribution function for finite systems *J. Math. Phys.* **39** 6247–61
[36] Ali S T, Atakishiyev N M, Chumakov S M and Wolf K B 2000 The Wigner function for general Lie groups and the wavelet transform *Ann. Henri. Poincaré* **1** 685–714